J Mater Sci (2009) 44:5900–5908
DOI 10.1007/s10853-009-3835-7

Effect of iron doping on magnetic properties of $Sr_{0.78}Y_{0.22}CoO_{2.625+\delta}$-layered perovskite

I. O. Troyanchuk · D. V. Karpinsky · A. P. Sazonov · V. Sikolenko · V. Efimov · A. Senyshyn

Received: 24 February 2009 / Accepted: 21 August 2009 / Published online: 1 September 2009

Abstract The $Sr_{0.78}Y_{0.22}Co_{1-x}Fe_xO_{2.625+\delta}$ ($x = 0$ and 0.12) system has been studied using neutron diffraction technique, magnetization, and elastic properties measurements. Undoped sample exhibits superstructure with $2\sqrt{2}a_p * 2\sqrt{2}a_p * 4a_p$ metrics and structural phase transition at $T = 360$ K. Magnetic ordering starts to develop below 360 K. Spontaneous magnetization shows anomalous behavior and reaches maximal value nearly room temperature. A magnetic structure of the both compounds has been described assuming G-type antiferromagnetic ordering. There are two different magnetic moment values for Co ions in CoO_6 and $CoO_{4.5}$ layers. Magnetic moments in $CoO_{4.5}$ layers are larger than those for octahedrons. The refined values of magnetic moments indicate a mixed low–high spin state of Co^{3+} for the both layers. There is no evidence for any change of the magnetic structure type with temperature lowering despite the anomalous magnetization behavior. Iron doping ($x = 0.12$) leads to a suppression of the small ferromagnetic component, disappearance of the $2\sqrt{2}a_p * 2\sqrt{2}a_p * 4a_p$ metrics, and strong increase of the average magnetic moment for $Co_{4.5}$ layer. It is suggested that the ferromagnetic component in the undoped samples is a result of non-collinearity of the magnetic moments within $CoO_{4.5}$ layers.

I. O. Troyanchuk · D. V. Karpinsky
Scientific-Practical Materials Research Centre NAS of Belarus, P. Brovka str. 19, 220072 Minsk, Belarus

A. P. Sazonov · A. Senyshyn
Technische Universität München, Forschungsneutronenquelle Heinz Maier-Leibnitz (FRM II), Lichtenbergstr. 1, 85748 Garching, Germany

V. Sikolenko · V. Efimov
Laboratory of Neutron Scattering, ETH Zurich and Paul Scherrer Institute, 5232 Villigen, Switzerland

D. V. Karpinsky (✉)
Department of Ceramics and Glass Engineering and CICECO, University of Aveiro, 3810-193 Aveiro, Portugal
e-mail: karpinski@ua.pt

Introduction

Perovskite related cobalt oxides attract a great attention due to a large variety of physical phenomena associated with spin-state transitions [1, 2] as well as an interplay between magnetic and transport properties [3, 4]. It is supposed that Co^{3+} ions can adopt a low spin state (LS), an intermediate (IS) or a high spin one (HS). Since these states are very close in energy they can be changed by temperature, pressure or external magnetic field. Actually in [5] a pressure-induced transition into an insulating LS state was found for $La_{1-x}Sr_xCoO_3$ system. Usually low-temperature or high-pressure phases favor LS state whereas temperature increase or decrease of "chemical" pressure leads to the transition into HS state.

Recently discovered layered perovskites with a chemical formula $Sr_{0.75}Ln_{0.25}CoO_{2.625}$ ($Sr_3LnCo_4O_{10.5}$) exhibit spontaneous magnetization up to 335 K. The cobalt ions adopt 3+ oxidative state [6, 7]. Above 500 K these compounds become metallic. The magnetization versus temperature dependence shows an anomalous behavior: spontaneous magnetization increases sharply with temperature increase [6–8]. According to [8] the spontaneous magnetization of $Sr_{0.75}Y_{0.25}CoO_{3-\gamma}$ at 4.2 K is about 0.05 μ_B whereas at 270 K it reaches value of about 0.7 μ_B per formula unit. It was suggested that the anomalous behavior of magnetization is a result of spin-state transition of the Co^{3+} ions: a large portion of Co^{3+} ions changes into

the non-magnetic LS state with temperature decrease. The ferromagnetism has been interpreted in terms of orbital ordering because a small amount of impurities (6% Mn ions doping) dramatically suppresses ferromagnetic properties [9]. This result cannot be explained by usual magnetic dilution effect.

The crystal structure of $Sr_{0.7}Y_{0.3}CoO_{2.62}$ compound has been refined in tetragonal space group *I4/mmm* with $2a_p * 2a_p * 4a_p$ unit cell [6]. According to [6] it contains layers of CoO_6 octahedrons alternatively with disordered oxygen-deficit layers of $CoO_{4.5}$ tetrahedrons and pyramids. Strontium and yttrium ions seem to be partially ordered. In [7] the crystal structure of $Sr_{1-x}Y_xCoO_{3-d}$ has been found to be strongly sensitive to yttrium content. In the range $0.15 \leq x \leq 0.25$ a new distortion of the crystal structure appears [7]. This structure was described in *Cmma* orthorhombic space group on $2\sqrt{2}a_p * 4a_p * 2\sqrt{2}a_p$ unit cell with additional oxygen ordering [7]. On the other hand synchrotron X-ray data of $Sr_{0.8}Er_{0.2}CoO_{3-d}$ crystal structure have been refined in monoclinic space group *A2/m* [9]. According to [9] this compound exhibits two structural phase transitions. The transition at $T = 509$ K is driven by oxygen vacancies ordering within $CoO_{4.5}$ layers whereas that at $T = 360$ K is ascribed to an orbital ordering.

In order to clarify the magnetic properties of $Sr_{1-x}Y_xCoO_{3-d}$ we have undertaken neutron diffraction study of $x = 0.22$ composition. The $x = 0.22$ value has been chosen because of mostly pronounced ferromagnetic properties at nearly this concentration [10]. It was shown that the magnetic structure is basic of G-type antiferromagnetic within a whole magnetically ordered range: the magnitude of the magnetic moment increases gradually with decreasing temperature despite an anomalous behavior of magnetization. We have found that the doping with iron leads to a suppression of the small ferromagnetic component, disappearance of the crystal structure phase transition at 360 K, and to strong increase of the magnetic moments value. However, the basic magnetic structure remains antiferromagnetic of G-type. The model of the non-collinear magnetic structure is proposed in order to explain the small ferromagnetic component and anomalous magnetization behavior.

Experimental

The slowly cooled and quenched samples $Sr_{0.78}Y_{0.22}CoO_{3-d}$ as well as slowly cooled $Sr_{0.78}Y_{0.22}Co_{0.88}Fe_{0.12}O_{3-d}$ one were synthesized from a stoichiometric mixture of $SrCO_3$, Y_2O_3, CoO, and Fe_2O_3. The mixtures were ground in a planetary mill "RETSCH" and sintered in air at $T = 1{,}400$ K for 3 h followed with cooling down to room temperature with a rate of 100̊/h. The quenched sample was prepared by removing a crucible from a furnace immediately after synthesis. Phase analysis of the products was made with DRON-3M X-ray diffractometer with Cu-Kα radiation. Elastic properties were measured using a resonance method at low frequency ($\nu \sim 10$ kHz). Neutron diffraction data were collected using high-resolution powder diffractometer (FIREPOD, E9) at the Helmholtz Centre Berlin for Materials and Energy (BENSC, Berlin) with a wavelength of 1.797 Å as well as SPODI instrument with 1.549 Å wavelength at Forschungsneutronenquelle Heinz Maier-Leibnitz (FRM II, München). The undoped sample was also studied at the spallation neutron source SINQ at the Paul Scherrer Institute using a high-intensity diffractometer DMC ($\lambda = 2.45$ Å). Data analysis was performed using FullProf software package. The magnetization measurements were taken out using MPMS-5 magnetometer (Quantum Design).

Results and discussion

Magnetization and elastic properties measurements

Figure 1 shows temperature dependences of magnetization for $Sr_{0.78}Y_{0.22}Co_{1-x}Fe_xO_{3-d}$ samples. The measurements were taken at 300 Oe on warming after cooling in a field (FC) and after cooling in zero field (ZFC). The spontaneous magnetization develops practically at the same temperature (350 K) for slowly cooled and quenched compounds, a

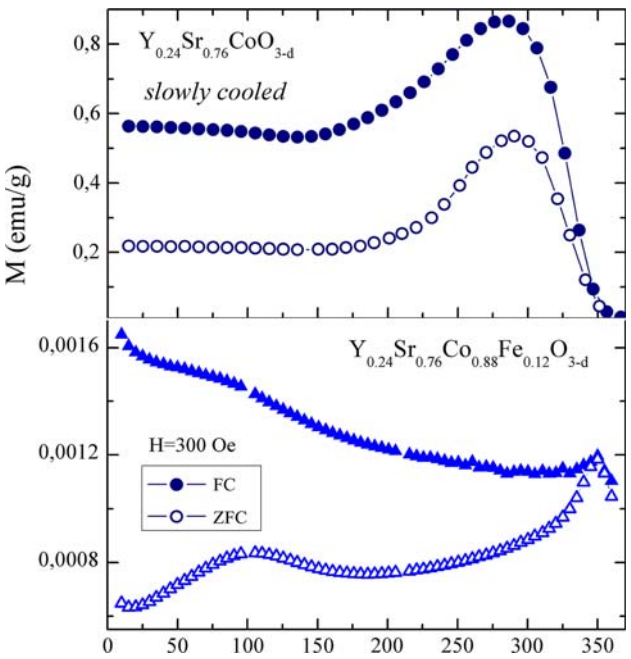

Fig. 1 Temperature dependences of the magnetization for the slowly cooled and the Fe-doped compounds measured in the FC and ZFC modes at $H = 300$ Oe

Fe-doped compound reveals a cusp-like magnetic anomaly near this temperature. Both FC and ZFC magnetizations exhibit maxima about room temperature. A large difference between ZFC and FC magnetizations was observed in fields up to 10 kOe. The magnetic hysteresis loops are illustrated in Fig. 2. A large coercive field indicates that $Sr_{0.78}Y_{0.22}CoO_{3-d}$ is a hard magnetic material. The magnetization is not saturated in fields up to 5 T at room temperature so it is difficult to determine the spontaneous magnetization correctly. It is worthy to be noted that second cycle of M(H) measurement leads to a larger value of the magnetic moment than that observed for the first cycle. One can state that the spontaneous magnetization at 300 K is not less than $M = 0.20\ \mu_B$ per Co ion for the slowly cooled sample. The quenched sample shows about twice as smaller spontaneous magnetization, however, the coercive field at room temperature is certainly larger than for slowly cooled compound. Coercive field at liquid helium temperature is not less than 10 kOe. Both the slowly cooled and quenched samples exhibit a pronounced decrease of the spontaneous magnetization as temperature lowers from 290 K to 5 K (Fig. 2). Field isothermal magnetization dependences are practically linear for the iron-doped

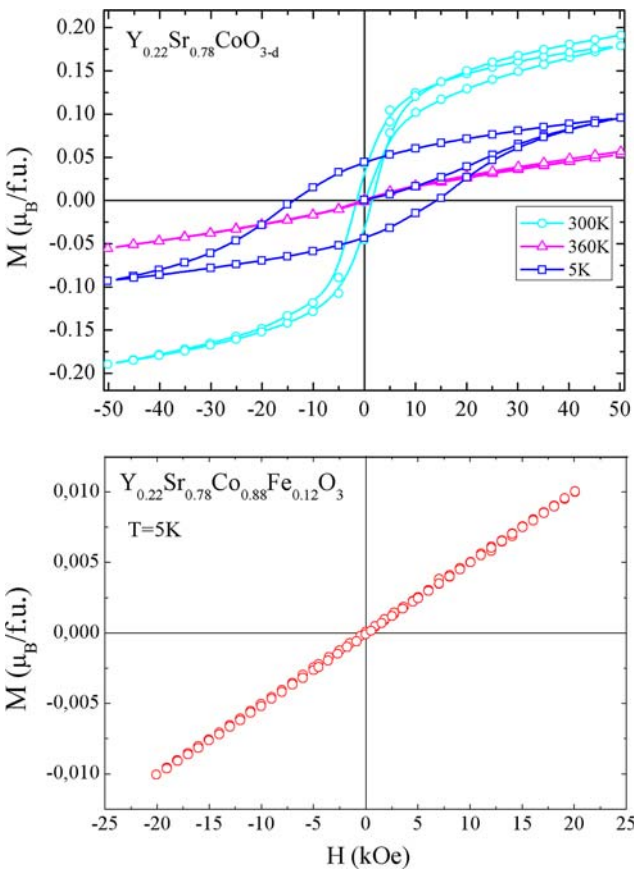

Fig. 2 Isothermal magnetization for the slowly cooled and the Fe-doped compounds

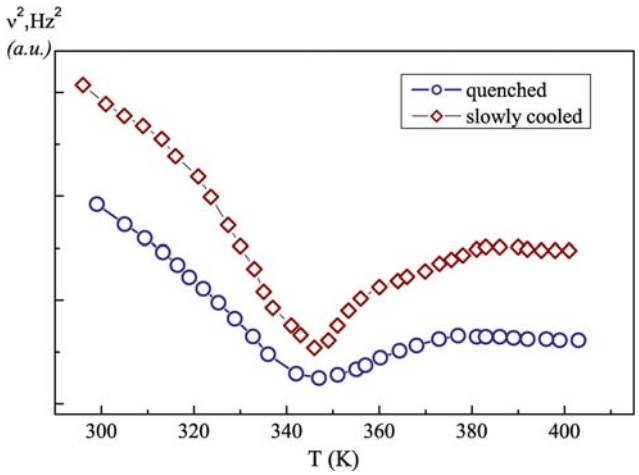

Fig. 3 Temperature dependences of Young modulus for the slowly cooled and the quenched compounds

sample (Fig. 2) as it is expected for the antiferromagnetic state. However, ZFC and FC magnetizations do not coincide below 350 K thus indicating a presence of the very small spontaneous magnetization. The measurement of elastic properties of the $x = 0$ sample shows that at 350 K there is a minimum of Young modulus (Fig. 3). Such a behavior can be interpreted in terms of the structural phase transition coinciding with onset of magnetic ordering. No anomalous behavior of elastic properties was revealed for the Fe-doped sample.

Crystal and magnetic structures study

Crystal structure refinement for $Sr_{0.22}Y_{0.78}CoO_{3-d}$ and $Sr_{0.78}Y_{0.22}Co_{0.88}Fe_{0.12}O_{3-d}$ compounds has been performed based on neutron diffraction measurements. The NPD patterns have been recorded in the temperature range of 5–450 K. The crystal structure of the Fe-doped sample at 450 K has been refined using the orthorhombic space group *Immm* with $2a_p * 2a_p * 4a_p$ unit cell in the single phase model (see inset of Fig. 4). The refinement of the crystal structure within tetragonal *I4/mmm* space group gave slightly worse reliability factors. The crystal structure parameters are presented in the Table 1. According to the refinement the unit cell contains an alternating linkage of the layers of oxygen octahedrons CoO_6 and layers of pyramids $CoO_{4.5+\delta}$ arranged along *c*-axis. The pyramids have substantially distorted structure and a good deal of oxygen vacancies. An essential distortion of oxygen octahedrons arranged around Co ions in *8k* site is caused by a high concentration of oxygen vacancies in *4e* sites of oxygen ions. Symmetry operations allowed for the latter crystallographic position provide an alternation of oxygen polihedra arrangement along *c*-axis.

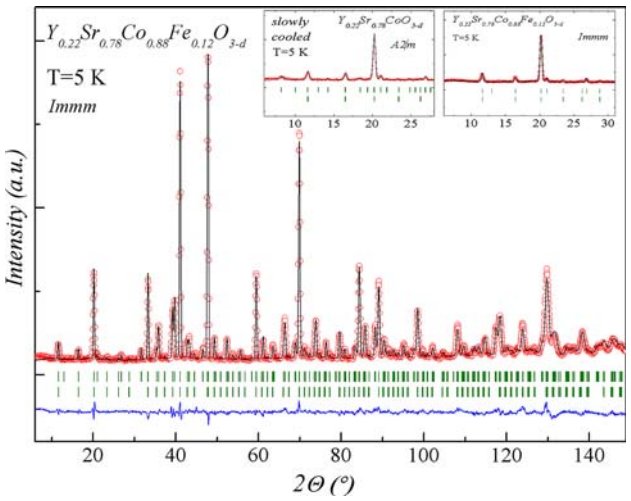

Fig. 4 NPD refined pattern for the Fe-doped compound at 5 K measured using SPODI instrument. The observed intensities are shown by *dots* and the calculated ones by *solid line*. The positions of the Bragg reflections are shown by the small *vertical lines* below the patterns (the *upper line* denotes crystallographic phases (*Immm*) the lower one marks magnetic phase of G-type). Magnified small angle patterns for the slowly cooled and the doped compounds are shown at the inset

A set of the weak additional peaks has been observed on NPD patterns for the undoped slowly cooled and the quenched samples. The intensities of superstructure peaks for the quenched sample are lower than for the slowly cooled one. These reflections are indexed on the base of $2\sqrt{2a_p} * 2\sqrt{2a_p} * 4a_p$ unit cell (Fig. 4). Some of the superstructure reflections have been observed above magnetic transition temperature that exclude their magnetic origin. So these reflections are a result of crystal structure transformation. According to [7] the crystal structures of $Sr_{0.8}Ln_2CoO_{3-d}$ can be described in orthorhombic space group *Cmma* with $2\sqrt{2a_p} * 2\sqrt{2a_p} * 4a_p$ supercell. However, we failed to refine the crystal structure in the single phase model using *Cmma* space group. The attempts to refine the crystal structure using monoclinic *A2/m* space group gave relatively large factors of reliability ($\chi \sim 10$), so the crystal parameters are not presented in the Table 1. According to [9] the crystal structure transition at $T = 360$ K leads to further increase of unit cell up to $4\sqrt{2a_p} * 2\sqrt{2a_p} * 4a_p$ metrics. However, we did not observe any peaks associated with this type of unit cell apparently due to very small intensities. The crystal structure of Fe-doped sample at 2 K was refined on the base of *Immm* space group because there was no indication of any crystal structure transition below 450 K.

Based on NPD investigations an oxygen content value for the Fe-doped compound is about 2.65, whereas for the undoped one this value is close to ~2.63. Assuming the results obtained one can suppose that almost all Co ions are in 3+ oxidative state, Fe ions in similar solid solutions also adopt an oxidative state 3+ [11, 12]. Spin and oxidative states of Co and Fe ions essentially govern a magnetic structure of the compounds.

Analysis of NPD data at low temperatures leads to conclusion that reflections (112), (132), (332) give a main magnetic contribution, where indexes refer to $2a_p * 2a_p * 4a_p$ unit cell. These reflections start to develop slightly below 360 K for the slowly cooled Fe-free sample. It means that the basic magnetic structure for all the compounds can be described with a simple $2a_p * 2a_p * 2a_p$ unit cell assuming the G-type antiferromagnetic ordering. However, analysis of the magnetic peak intensities ratio testifies that the magnetic structure of the compounds is not pure G-type one with equal moments for CoO_6 and $CoO_{4.5}$ layers. Therefore a magnetic structure refinement has been performed in a model with different magnitudes of magnetic moments for CoO_6 and $CoO_{4.5}$ layers. It was found that the magnetic moments in octahedra are smaller than those in $CoO_{4.5}$ layers. In comparison with $Sr_{0.78}Y_{0.22}CoO_{2.63}$ compounds for $Sr_{0.78}Y_{0.22}Co_{0.88}Fe_{0.12}O_{2.65}$ a difference between magnetic moments is more pronounced and magnetic moments are noticeably larger (see Table 1 and Fig. 5).

A magnetic structure refinement in a model where magnetic moments are co-directionally aligned with *a, b* lattice axes did not allow to fit the (110) reflection (at about 16.5°). Reliability factors improvement for all the NPD patterns has been achieved in a model with ordered magnetic moments along *c* lattice axis. Magnetic structure of the compounds can be described in terms of two antiferromagnetic sublattices with different magnetic moment values.

We did not observe any ferromagnetic contribution in a magnetic neutron scattering. Apparently this contribution is too small to be revealed by standard NPD method. All magnetic peaks do not show anomalous behavior with temperature lowering (Fig. 5). The magnetic moments in both $CoO_{4.5}$ and CoO_6 layers gradually increase as temperature decreases despite anomalous magnetization behavior. These data are incompatible with temperature driven transition of cobalt ions from high to low spin state proposed in [8] to explain the drop of magnetization with temperature decreasing.

There are two different models of magnetic structure to explain the origin of the ferromagnetic component revealed with magnetization measurements. The first one suggests a collinear ferrimagnetic ordering within $CoO_{4.5}$ layers. The space group *A2/m* allows two non-equivalent crystallographic positions within $CoO_{4.5}$ layers. The magnetic moments of Co^{3+} associated with these positions are different so the antiferromagnetic coupling between them should lead to non-compensated magnetic moment. However, in frame of this model it is difficult to explain the anomalous increase of magnetization with increasing

Table 1 The results of crystal and magnetic structure refinement of the NPD data

Atom	Parameter	Slowly cooled		12% Fe			
		5 K *A2/m*	450 K *I4/mmm*	5 K *Immm*	450 K *Immm*	5 K *I4/mmm*	450 K *I4/mmm*
	a, Å	10.8564	7.6558	7.6571	7.66431	7.6517	7.6681
	b, Å	10.8692	7.6558	7.6448	7.67283	7.6517	7.6681
	c, Å	15.3428	15.3997	15.2876	15.40677	15.2853	15.4072
	c/2a		1.006			0.9988	1.004
	Volume, Å	**1810.47 (56.57)**	**902.59 (56.41)**	**894.93 (55.93)**	**906.04 (56.63)**	**894.93 (55.93)**	**905.93 (56.62)**
Sr(1)/Y(1)	(Wyck.)		*4e*	*4i*		*4e*	
	X		0	0	0	0	0
	Y		0	0	0	0	0
	Z		0.8783	0.8677	0.8659	0.8772	0.8780
	Biso, Å^2		0.6	1.0	1.9	1.1	1.4
	occ.						
Sr(2)/Y(2)				*4j*		*8g*	
	X		0	0.5	0.5	0	0
	Y		0.5	0	0	0.5	0.5
	Z		0.8683	0.3506	0.3518	0.8693	0.8692
	Biso, Å^2		0.9	1.0	0.7	1.1	1.2
	occ.						
Sr(3)/Y(3)				*4j*		*4e*	
	X		0	0	0	0	0
	Y		0	0	0	0	0
	Z		0.3525	0.1233	0.1220	0.3524	0.3529
	Biso, Å^2		0.8	0.5	0.9	0.6	0.7
	occ.						
Sr(4)/Y(4)				*4i*			
	X		–	0	0	–	–
	Y		–	0	0	–	–
	Z		–	0.3693	0.3704	–	–
	Biso, Å^2		–	0.9	0.8	–	–
	occ.						
Co(1)				*8n*		*8h*	
	X		0.7525	0.7562	0.7566	0.7493	0.7472
	Y		0.7525	0.2472	0.2498	0.7493	0.7472
	Z		0	0	0	0	0
	Biso, Å^2		1.2	0.7	1.1	0.9	0.7
	occ.						
Co(2)				*8k*		*8f*	
	X		0.25	0.25	0.25	0.25	0.25
	Y		0.75	0.75	0.75	0.75	0.75
	Z		0.25	0.25	0.25	0.25	0.25
	Biso, Å^2		1.0	0.7	0.5	0.7	0.7
	occ.						
O(1)				*8l*		*16n*	
	X		0	0	0	0	0
	Y		0.2456	0.2607	0.25283	0.2464	0.2458
	Z		0.2416	0.2575	0.25842	0.2402	0.2417

Table 1 continued

Atom	Parameter	Slowly cooled		12% Fe			
		5 K *A2/m*	450 K *I4/mmm*	5 K *Immm*	450 K *Immm*	5 K *I4/mmm*	450 K *I4/mmm*
	Biso, Å^2		1.2	0.8	0.7	0.8	0.9
	occ.		0.97			1.0	1.0
O(2)				*8m*		*16m*	
	X		0.2823	0.2453	0.25508	0.2848	0.2851
	Y		0.2823	0	0	0.2848	0.2851
	Z		0.1181	0.2394	0.2408	0.1165	0.1167
	Biso, Å^2		2.3	0.7	1.0	2.0	2.2
	occ.		1.0			1.0	1.0
O(3)				*16o*		*8i*	
	X		0	0.2176	0.2139	0	0
	Y		0.7238	0.2879	0.2855	0.7292	0.7223
	Z		0	0.1172	0.1171	0	0
	Biso, Å^2		1.6		1.9	1.3	1.5
	occ.		0.98			1.0	1.0
				4e		*8j*	
O(4)			0.3675	0	0	0.3875	0.3857
	X		0.5	0.6505	0.7682	0.5	0.5
	Y		0	0	0	0	0
	Z		3.1	1.2	1.2	2.7	2.9
	Biso, Å^2		0.26			0.32	0.32
	occ.						
O(5)				*4g*			
	X			0.7596	0.7614	–	–
	Y			0	0	–	–
	Z			0	0	–	–
	Biso, Å^2			1.3	2.7	–	–
	occ.						
O(6)				*4f*			
	X			0.1234	0.1115	–	–
	Y			0.5	0.5	–	–
	Z			0	0	–	–
	Biso, Å^2			6.0	4.0	–	–
	occ.						
O(7)				*4h*			
	X			0.5	0.5	–	–
	Y			0.7204	0.7042	–	–
	Z			0	0	–	–
	Biso, Å^2			0.4	0.8	–	–
	occ.						
		Co_{pent} (1)–O(2), Å		Co(1)–O(3), Å		Co_{pent} (1)–O(2), Å	
			1.858(5)	1.830	1.839	1.819(3)	1.835(3)
		Co_{pent} (1)–O(3), Å		Co(1)–O(6), Å		Co_{pent} (1)–O(3), Å	
				2.143	2.168		
			1.906(6)	Co(1)–O(7), Å		1.924(5)	1.947(3)
		Co_{pent} (1)–O(4), Å		1.977	1.999	Co_{pent} (1)–O(4), Å	
			2.142(8)	Co(1)–O(5), Å		2.174(8)	2.147(8)

Table 1 continued

Atom	Parameter	Slowly cooled		12% Fe			
		5 K *A2/m*	450 K *I4/mmm*	5 K *Immm*	450 K *Immm*	5 K *I4/mmm*	450 K *I4/mmm*
		Co_{oct}(2)–O(1), Å		1.890	1.917	Co_{oct}(2)–O(1), Å	
			1.918(4)	Co(1)–O(4), Å		1.919(2)	1.921(2)
		Co_{oct}(2)–O(2), Å		2.03	1.870	Co_{oct}(2)–O(2), Å	
			2.061(5)	Co(2)–O(3), Å		2.075(3)	2.086(3)
				2.066	2.084		
		Co(2)–O(1)–Co(2)		Co(2)–O(2), Å		Co(2)–O(1)–Co(2)	
	Co1–O4		166.71(6)	1.9184	1.9238	170.82(2)	169.10(3)
		Co(1)–O(3)–Co(1)		Co(2)–O(1), Å		Co(1)–O(3)–Co(1)	
	Co1–O5	168.13(2)	172.01(2)	1.9194	1.9206	170.61(4)	169.12(3)
	Co1–O6			Co(2)–(O2)–(Co2)			
	Co1–O7			170.07	171.23		
	Co2–O1			Co(1)–(O4)–(Co1)			
	Co2–O2			156.0	171.6		
				Co(2)–(O1)–(Co2)			
				170.98	172.17		
				Co(1)–(O5)–(Co1)			
				179.2	177.8		
R_p (%)/R_{wp} (%)		**5.27/6.80**	**4.44/5.79**	**4.23/5.41**	**3.73/4.82**	**4.88/6.13**	**3.89/5.15**
R_{Bragg} (%)		**9.5**	**10.9**	**8.5**	**9.11**	**11.0**	**9.17**
χ^2		**6.96**	**5.62**	**4.85**	**3.94**	**6.13**	**4.47**
Magnetic moment Co(Fe), μ_B							
G-type		tetr		tetr		tetr	
		$M_{gen} = \pm 2.2\ \mu_B$		$M_z = \pm 2.8\ \mu_B$		$M_z = \pm 2.8\ \mu_B$	
		oct		oct		oct	
		$M_{gen} = \pm 1.4\ \mu_B$		$M_z = \pm 1.6\ \mu_B$		$M_z = \pm 1.6\ \mu_B$	
Magnetic *R*-factor		**11.2**				**9.1**	

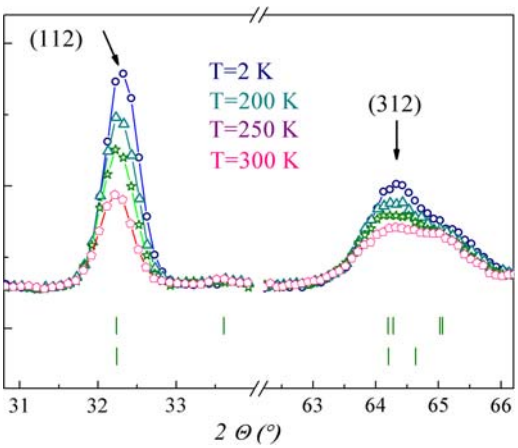

Fig. 5 Temperature evolutions of the main antiferromagnetic peaks for $Sr_{0.78}Y_{0.22}CoO_{2.63}$ sample. The NPD data were obtained using DMC instrument

temperature because neutron diffraction studies did not reveal any change of the basic G-type magnetic structure in all the temperature range of magnetic ordering.

Another magnetic structure model which is adjusted with NPD results assumes a canting of Co ions magnetic moments settled in $CoO_{4.5}$ layers. This magnetic structure provides an uncompensated magnetic moment arranged along *b*- or *a*-axes of the perovskite lattice. The latter proposed model of magnetic structure is in accordance with M(H) magnetic measurements for the slowly cooled and the quenched $Sr_{0.78}Y_{0.22}CoO_{2.63}$ compounds. In this model the anomalous magnetization versus temperature behavior (Figs. 1, 2) can be ascribed to a phase transition from a collinear to a non-collinear magnetic structure which does not affect strongly the basic antiferromagnetic G-type structure because ferromagnetic component is relatively small. So this model is more attractive in comparison with

ferrimagnetic one. However, the anomalous behavior of magnetization for samples studied in this work is much less pronounced than that for sample studied in [8] therefore further investigations are desirable.

Magnetic properties of $Sr_{0.78}Y_{0.22}Co_{0.88}Fe_{0.12}O_{2.65}$ compound can be well described within the collinear magnetic structure with different magnetic moments for $CoO_{4.5}$ and CoO_6 layers because there is no appreciable spontaneous magnetization in all the temperature range of magnetic ordering.

The ferromagnetic component observed in layered cobaltites is not result of Dzyaloshinsky–Moriya type magnetic interactions as it is commonly accepted for $LnMO_3$ (Ln = lanthanide; M = Fe, Mn, V) perovskites. In these perovskites a ferromagnetic component does not exceed 0.05 μ_B whereas for layered cobatites it can reach about 0.7 μ_B [8]. In order to understand an origin of the non-collinear magnetic structure it is necessary to consider exchange interactions in $CoO_{4.5}$ layer. We suppose exchange interactions in this sublattice to be negative in the case when nearest pyramids have common oxygen ion and positive if not. In this case all the interactions within *bc* plane are negative whereas along *a*-axis negative and positive ones are alternated. This leads to a frustration of the magnetic interactions and the non-collinear magnetic structure in the some temperature range could be more favorable than the simple collinear one. Doping with Fe^{3+} stabilizes the collinear antiferromagnetic G-type structure because the interactions Fe^{3+}–Fe^{3+} and Fe^{3+}–Co^{3+} seem to be strongly antiferromagnetic.

Results of a refinement of *8n* and *8k* position occupations (*Immm* space group model) testify a random distribution of Fe ions between mentioned crystallographic sites. Nevertheless magnetic moments of Co and Fe ions in *8h* (pentahedral coordination) are essentially more than those for *8f* sites (octahedral coordination) (see Table 1). It should be noted that for undoped compounds the difference between $CoO_{4.5}$ and CoO_6 magnetic moments is less pronounced (see Table 1). Moreover a relatively small substitution with iron leads to a substantial increase of the magnetic moments. Apparently the increase of the magnetic moments for the Fe-doped sample may be understood taking into account that this sample does not exhibit ferromagnetic component which should decrease antiferromagnetic one for undoped sample.

The magnetic moment value in the $CoO_{4.5}$ sublattice of the Fe-doped compound is 2.8 μ_B per ion. This value is significantly more than 2 μ_B associated with intermediate spin state. It was found that magnetic moments of the high-spin Co^{3+} ions in $Sr_2Co_2O_5$ and $BiCoO_3$ are 3.3 and 3.4 μ_B, respectively [13, 14]. However, the magnetic moment of the Co^{3+} ion in high-spin state ($S = 2$) should be about 4 μ_B. It is much above observed value even for Fe-doped sample. In contrast the magnitude of the magnetic moments in octahedra (1.4–1.6 μ_B) is much lower than expected ones for intermediate spin state (see Table 1). So, present data can hardly be adjusted with a pure ionic model for Co ions magnetic moments. In works [1, 15] Co^{3+} ions in $LaCoO_3$ have been shown to have first excited state corresponding to the high-spin one. Probably it is correct for $Sr_3LnCo_4O_{10.5}$ type compounds. Hence the description of the magnetic state of Co^{3+} ions in layered cobaltites could be done in terms of a mixed low–high spin magnetic state. In should be noted that according to photoemission study [16] e_g and t_{2g} electrons of Co^{3+} ions are delocalized even in insulating phase of $LnBaCo_2O_{5.5}$-layered cobaltites which exhibit similar magnetic properties [3, 4, 17]. Therefore using of itinerant magnetism approach seems to be more appropriate for description of the magnetic state.

In [9] it was suggested that the crystal structure phase transition at 360 K can result from the orbital ordering. The data received in the present work do not contradict this hypothesis. Apparently orbital ordering is associated with altering of d_{yz} and d_{xz} orbitals of Co^{3+} ions settled within $CoO_{4.5}$ layers along *a*-axis. This alteration leads to doubling of the unit cell along *a*-axis which was observed in [9]. It should be mentioned that similar orbital ordering has been proposed for $LnBaCo_2O_{5.5}$-layered perovskites below metal–insulator transition [17]. These compound doped with iron (4–5%) exhibit also antiferromagnet–"ferromagnet" transition, however, both antiferromagnetic and "ferromagnetic" phases have similar G-type antiferromagnetic structure [18]. Apparently a small ferromagnetic component is associated with non-collinear magnetism for both $LnBaCo_2O_{5.5}$- and $Sr_3LnCo_4O_{10.5}$-layered perovskites.

Summary

Effect of Fe doping on crystal and magnetic structures of $Sr_{0.78}Y_{0.22}CoO_{3-d}$-layered perovskites has been experimentally studied. It was shown that basic $Sr_{0.78}Y_{0.22}CoO_{3-d}$ compounds are antiferromagnetically ordered below T_N = 350 K. At T_N structural transition was found out apparently caused with orbital ordering in $CoO_{4.5}$ layers. A small ferromagnetic component was revealed by magnetization measurements with maximum of 0.2 μ_B per cobalt ion about room temperature. The basic antiferromagnetic structure is G-type; magnetic moments in CoO_6 and $CoO_{4.5}$ layers gradually increase with temperature decreasing despite the anomalous magnetization behavior. In all the studied temperature range (2–450 K) $Sr_{0.78}Y_{0.22}CoO_{3-d}$ exhibits superstructure $2\sqrt{2}a_p * 2\sqrt{2}a_p * 4a_p$-type apparently due to oxygen vacancy ordering in $CoO_{4.5}$ layers. The Fe-doped compounds are also G-type antiferrromagnetically ordered at T_N = 350 K, however, ferromagnetic component and structural transition at 350 K are absent. This compound

does not exhibit superstructure of $2\sqrt{2}a_p * 2\sqrt{2}a_p * 4a_p$-type.

It is suggested that ferromagnetic component is result of canting magnetic moments in $CoO_{4.5}$ layers due to orbital ordering. In this model the anomalous behavior of magnetization is associated with a temperature driven collinear–non-collinear magnetic structure phase transition. The refined values of magnetic moment for $CoO_{4.5}$ layers are 2.2 and 2.8 μ_B for undoped and Fe-doped compounds, respectively whereas for CoO_6 sublattice these values are 1.4 and 1.6 μ_B. For Co^{3+} in intermediate and high spin states the expected magnetic moments are 2 and 4 μ_B, respectively, therefore mixed spin state for Co ions is suggested.

Acknowledgements The work was supported partly by Fund for fundamental research of Belarus (project F08R-081) and by the European Commission under the 6th Framework Program through the Key Action: Strengthening the European Research Area, Research Infrastructures. Contract n: RII3-CT-2003-505925 (NMI3). One of the authors (D.V.K.) is grateful to the Foundation for Science and Technology of Portugal (FCT) for financial support (Grant No. SFRH/BPD/42506/2007).

References

1. Haverkort MW, Hu Z, Cezar JC, Burnus T, Hartman H, Reuther M, Zobel M, Lorenz T, Tanaka A, Brookes NB, Hsieh HH, Lin H-J, Chen CT, Tjeng LH (2006) Phys Rev Lett 97:176405
2. Wu J, Lynn JW, Glinka CJ, Burley J, Zheng H, Mitchell JF, Leighton C (2008) Phys Rev Lett 94:037201
3. Martin C, Maignan A, Pelloquin D, Nguyen N, Raveau B (1997) Appl Phys Lett 71:1421
4. Troyanchuk IO, Kasper NV, Khalyavin DD, Szymczak H, Szymczak R, Baran M (1998) Phys Rev Lett 80:3380
5. Lengsdorf R, Ait-Tahar M, Saxena SS, Ellerby M, Khomskii DI, Micklitz H, Lorenz T, Abd-Elmeguid MM (2004) Phys Rev B 69:1140403
6. Istomin SYa, Grins J, Swensson G, Drozhzhin OA, Kozhevnikov VL, Antipov EV, Attfield JP (2003) Chem Mater 15:4012
7. James M, Avdeev M, Barnes P, Morales L, Wallwork K, Withers R (2007) J Solid State Chem 180:2233
8. Kimura S, Maeda Y, Kashiwagi T, Yamaguchi H, Hagiwara M, Yoshida S, Terasaki I, Kindo K (2008) Phys Rev B 78:180403(R)
9. Ishiwata Sh, Kobayashi W, Terasaki I, Kato K, Takata M (2007) Phys Rev B 75:220406(R)
10. Kobayashi W, Yoshida Sh, Terasaki I (2006) J Phys Soc Jpn 75:103702
11. Lindberg F, Drozhzhin OA, Istomin SYa, Svensson G, Kaynak FB, Svendlindh P, Warnicke P, Wannberg A, Mellergard A, Antipov EV (2006) J Solid State Chem 179:1434
12. Bréard F, Maignan A, Lechevallier L, Boulon M-E, Le Breton JM (2006) Solid State Sci 8:619
13. Rodriguez J, Gonzalez-Calbet JM, Grenier JC (1987) Solid State Commun 62:231
14. Belik A, Iikubo S, Kadama K, Igawa N, Shamoto S, Niitaka S, Azuma M, Shimakawa Y, Takano M, Izumi F, Takayama-Muromachi E (2006) Chem Mater 18:798
15. Podlesnyak A, Streule S, Mesot J, Medarde M, Pomjakushina E, Conder K, Tanaka A, Haverkort MW, Khomskii DI (2006) Phys Rev Lett 97:247208
16. Takubo K, Son J-Y, Mizokawa T, Soda M, Sato M (2006) Phys Rev B 73:075102
17. Garcia-Fernandez M, Scagnoli V, Staub U, Mulders AM, Janousch M, Bodenthin Y, Meister D, Patterson BD, Mirone A, Tanaka Y, Nakamura T, Grenier S, Huang Y, Conder K (2008) Phys Rev B 78:054424
18. Troyanchuk IO, Karpinsky DV, Yokaichiya F (2008) J Phys Condens Matter 20:335228